International Conference on Applied Energy 2019
Aug 12-15, 2019, Västerås, Sweden
Paper ID: 0166

MODELLING AND EXPERIMENTAL VALIDATION OF DEPOSIT FORMATION FOR A WOODCHIP FIRED GRATE BOILER BASED ON A MECHANISTIC FOULING MODEL

Zhimin Zheng[1,2], Wenming Yang[1,2*], Hui Wang[3], Anqi Zhou[1,2], Yongtie Cai[1,2], Guang, Zeng[1,2], Hongpeng Xu[1,2]

1 Sembcorp-NUS Corporate Laboratory, Block E1A, #04-01, 1 Engineering Drive 2, 117576, Singapore.
2 Department of Mechanical Engineering, National University of Singapore, Block EA, #07-08, 9 Engineering Drive 1,117575, Singapore.
3 School of Energy Science and Engineering, Harbin Institute of Technology,92, West Dazhi Street, Harbin 150001, PR China; (Wenming Yang)

ABSTRACT

Woodchip as an alternative fuel is widely fired to generate electricity and steam. However, fouling is a major issue for woodchip fired boilers. It is important to develop mathematical models and predictive tools to understand and predict ash deposition behavior. A mechanistic fouling model considering build-up and removal mechanisms during ash deposition is developed in this work. In the models, the effect of surface roughness on ash deposition was also considered. Meanwhile, the fouling model was implemented into the ANSYS FLUENT and was combined with the discrete particle model (DPM), heat transfer model, and dynamic mesh model to predict ash deposition behavior on a deposition probe. The simulation result was validated against the experimental data obtained from a lab-scale experimental setup. The simulated trend of the deposit thickness as a function of time shows good agreement with the experimental results. Based on the developed model, the effects of the removal model and flue gas velocity were investigated. The results show that it is necessary to consider the removal mechanism even when the flue gas is low. The deposition mass presented a significant decrease with the increase of flue gas velocity. An asymptotic trend for the deposition mass was observed for the cases considering the removal model. The research shows that the mechanistic fouling model coupled with CFD is a promising tool to predict the ash deposition behavior in low-temperature conditions for the woodchip fired grate boilers.

Keywords: ash deposition; grate boiler; woodchip; dynamic mesh; dynamic simulation; surface roughness

1. INTRODUCTION

Wood fuel as an alternative fuel has been widely accepted in many countries. However, the issue like slagging and fouling is one of the most challenge problems faced by these biomass boilers. Many researchers focusing on ash deposition problems are developing models and predictive tools to understand and predict ash deposition behavior by numerical methods and have made much attempt to find effective solutions to minimize ash deposition issues.

Ash deposition models attract the most attention from numerical researchers because it directly determines the reliability and accuracy of simulation results. Many theoretic models have been developed to describe the deposition probabilities. Generally, there are three types of ash deposition models: viscosity-based model [1], melting fraction-based model [2], and critical velocity-based model [3]. The first two types of ash deposition models mentioned above are usually available to predict ash deposition behavior under high -temperature conditions. However, the nature of the critical velocity-based models is mechanistic and more complicated. Ash deposit removal is another important process during ash deposition. The removal mechanisms of ash deposit in coal-fired and biomass-fired combustion boilers were summarized by Zbogar et al [4]. It is known that fundamental experimental research on removal mechanism of ash deposit with respect to fouling or slagging issues in boilers is still lack.

Based on the literature review above, it is noted that critical velocity-based deposition models can give more details on the deposition process, compared to the other two types of ash deposition models. It is also more suitable to predict the formation of powdery deposit. The main objective of this research is to develop a mechanistic fouling model considering both ash deposition and removal processes to predict ash deposition behavior based on ANSYS FlUENT platform. Dynamic mesh method with a novel smooth strategy was used to simulate the shape of ash deposit. The simulation result was also validated against the experimental data obtained in a lab scale deposition experiment setup with an advanced measurement system. The effect of the velocity of flue gas on ash deposition was predicted. Wide applications of the developed approach in predicting the fouling issues can be foreseen in boilers.

2. METHODOLOGY

2.1 Experiments

A temperature controlled experimental setup is developed to carry out ash deposition experiments, as shown in Fig. 1. An advanced deposition probe is used to monitor the heat exchanger tube. The detailed information about the experimental setup and the probe can be found in literature [5]. The metal wall temperature of the probe can be auto-controlled by a temperature-controlled system[6]. Additionally, it should be emphasized that the effective thermal conductivity and surface temperature of ash deposit as a function of time can be obtained by further analyzing the experimental data.

2.2 Models

Main models used in this simulation includes DPM model, heat transfer model, ash deposition model, and dynamic mesh model. Detailed description is focused on the ash deposition model due to the space limitations. The relevant descriptions of other models can be found in literature [7].

2.2.1 A mechanistic fouling model

2.2.1.1 Ash deposition model

The schematic diagram of an incident particle impacting the substrate is shown in Fig. 2. $v_{n,I}$ and $v_{t,I}$ are the normal velocity and tangential velocity of the incident velocity $\vec{v}_I$, respectively. $v_{n,R}$ and $v_{t,R}$ are the normal velocity and tangential velocity of the rebound velocity, respectively. $\vec{v}_R$. θ_I and θ_R are the incident angle and rebound angle, respectively. The impacts can be divided into two cases: non-oblique impacts and oblique impacts, according to the incident angle of the incident particle.

For the cases of non-oblique impacts, a mechanistic model can be used to determine whether a particle sticks on the surface or rebounds [8]. When a particle impacts on a surface, it will deform against the surface upon the impaction. When the particle velocity reduces to zero, the energy conversation is expressed as:

$$Q_{k,I}+Q_{a,I}=Q_{el}+Q_{pl}+Q_{loss} \quad (1)$$

where $Q_{k,I}$ is kinetic energy; $Q_{a,I}$ is the adhesion

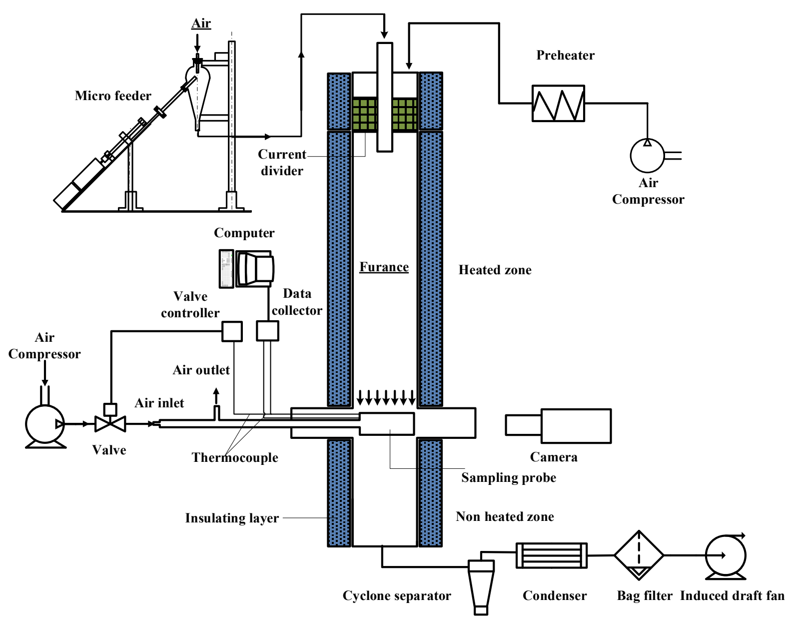

Fig. 1 Experiment setup

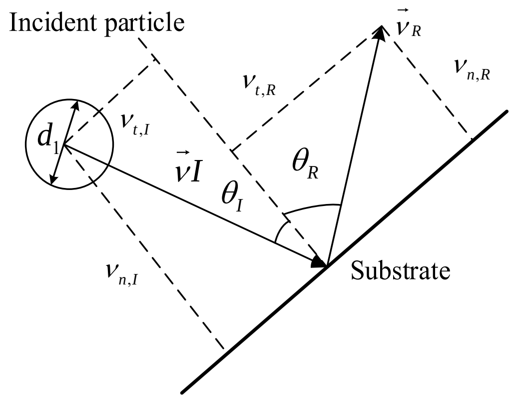

Fig. 2 The Schematic diagram of an incident particle impacting the substrate

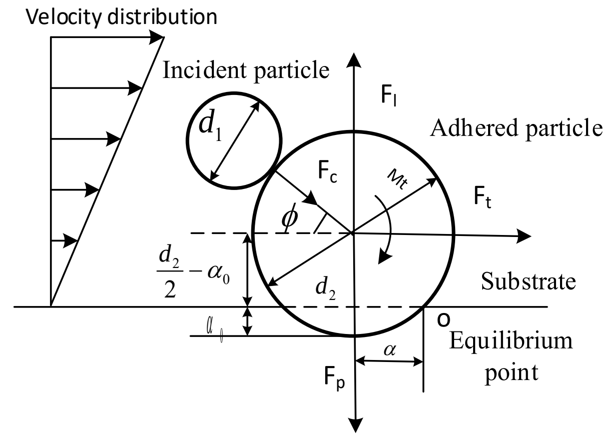

Fig. 3 Force analysis of an adhered particle in the shear flow field

energy of the approach phase; Q_{el} and Q_{pl} are the stored energy due to elastic deformation and plastic deformation, respectively; Q_{loss} is the loss of energy due to plastic material flow.

During the impaction process, two types of deformations for the incident particle may occur. A critical plastic-deformation velocity $v_{n,\lim}$ is used to determine the types of the deformation processes. If the normal impact velocity $v_{n,I}$ of the particle is smaller than $v_{n,\lim}$, it means only the elastic deformation occurs without considering the plastic deformation ($Q_{el}=Q_{pl}=0$). Otherwise, the plastic deformation should be also included. $v_{n,\lim}$ can be calculated by this equation [9]:

$$v_{n,\lim}=\frac{\pi^2}{\sqrt{10\rho_p}}\frac{(0.795Y)^{2.5}}{E^{*2}}\sqrt{\frac{1+C_m}{C_m}} \quad (2)$$

where Y is the limit elastic yield; ρ_p is the particle density; E^* is the effective Young's modulus, and C_m is the mass factor.

If the stored elastic energy is smaller than or equal to the adhesion energy of the restitution phase $Q_{A,R}$, the particle will stick on the surface. The following equation is taken as the sticking criterion. When

$$Q_{el}+Q_{pl}\le Q_{A,R} \quad (3)$$

Otherwise, the particle rebounds and the restitution coefficient e of the particle impaction is calculated by:

$$e=\sqrt{1-\frac{Q_{loss}+(Q_{A,R}-Q_{A,I})}{Q_{k,I}}} \quad (4)$$

where $Q_{A,I}$ is the adhesion energy of the approach phase.

The normal rebound velocity $v_{n,R}$ of the particle can be further obtained by

$$v_{n,R}=\sqrt{\frac{Q_{k,I}-Q_{loss}-(E_{A,R}-Q_{A,a})}{1/2m^*}} \quad (5)$$

The rebounding particle may rotate or slip after collision with the surface. If the friction coefficient f_s is larger than some value, it will rotate.

$$f_s>\frac{2\tan\theta_I}{7(1+e)} \quad (6)$$

The corresponding tangential rebound velocity can be calculated by

$$v_{t,R}=v_{t,I}(1-\frac{2}{7}\frac{C_m}{1+C_m}) \quad (7)$$

Otherwise, the particle slips and is calculated by

$$v_{t,R}=v_{t,I}(1-\frac{f(1+e)}{\tan\theta_I}\frac{C_m}{1+C_m}) \quad (8)$$

However, it has to be pointed out that the deposition model as described above will be inapplicable if the incidence angle θ_I is larger than a certain critical value θ_{cr}. No particle stuck on the surface for the very oblique impacts by the experimental observation [10]. The critical angle θ_{cr} is given as [10]:

$$\tan(\theta_{cr})\approx 6.547f\sqrt{\frac{2-2v}{2-v}} \quad (9)$$

To consider the effect of the roughness of the deposit surface on ash deposition, the impact angle is further corrected and can be expressed as [11]:

$$\theta'=\theta+\Delta r\xi \quad (10)$$

where θ' is the corrected impact angle of an incident particle with a rough surface, ξ is a Gaussian random variable with a mean of 0 and standard deviation of 1, and Δr can be determined by the following equation [12]:

$$\Delta r = k_0(\frac{\pi}{2} - \arccos(\frac{d_2}{d_2 + d_1})) \quad (11)$$

where k_0 is a constant and depends on the surface roughness. d_1, d_2 are the diameters of the incident particle and adhered particle, respectively.

2.2.1.2 Ash removal model

The removal mechanism can be explained by the force and moment analysis on the adhered particle in the shear flow field [13]. There are four main forces and hydrodynamic moment acting on the adhered particle in this model. These forces include adhesion force, impact force, drag force, and lift force. Gravitational force is neglected since it is very small compared to other forces.

As shown in Fig. 3**Error! Reference source not found.**, the adhered particle will roll from its equilibrium point and is detached from the surface of the substrate, if the external moment is greater than or equal to the moment due to the adhesion force. With respect to the point O, the criterion of rolling particle detachment is given as

$$M_t + F_t(\frac{d_2}{2} - a_0) + F_l\alpha_{Rough} + F_c[-\sin\phi(\frac{d_2}{2}\cos\phi + \alpha_{Rough}) + \cos\phi(\frac{d_2}{2}\sin\phi + \frac{d_2}{2} - a_0)] \geq F_{po}^{Rough}\alpha_{Rough} \quad (12)$$

where M_t is the hydrodynamic moment, F_t is the drag force, F_c is the impact force, F_{po}^{Rough} is the pull-off force for a rough spherical particle from a rough surface, d_2 is the diameter of the adhered particle, O is the equilibrium point, ϕ is the contract angle, α_0 is the relative distance between the particle and surface at equilibrium conditions, and α_{Rough} is the contact radius for rough particles.

Sliding particle detachment also occur if the friction force is overcome.

$$F_t + F_c\cos\phi \geq (F_{po}^{Rough} - F_l + F_c\sin\phi) f_s \quad (13)$$

2.2.2 *Coupling processes of ash deposition and removal*

The formation of ash deposit coupling ash deposition and removal process on a tube in a cross flow is illustrated in Fig. 4. Some particles impacting the surface of ash deposit or the clean tube will deposit on the surface or rebound off it. When an incident particle collides with an adhered particle, the adhered particle may be removed due to the impact of the incident particle. However, it needs to be noted that the surface of ash deposit is usually took as a smooth surface in CFD simulations. But the deposit surface is composed of particles with different particle sizes. Furthermore, a position information of the adhered particles is not known in 2D CFD simulations. Therefore, in order to couple the processes of ash deposition and removal in 2D CFD simulations, it is necessary to make some assumption.

It is here assumed that there is a virtual adhered particle located in the normal direction of the surface

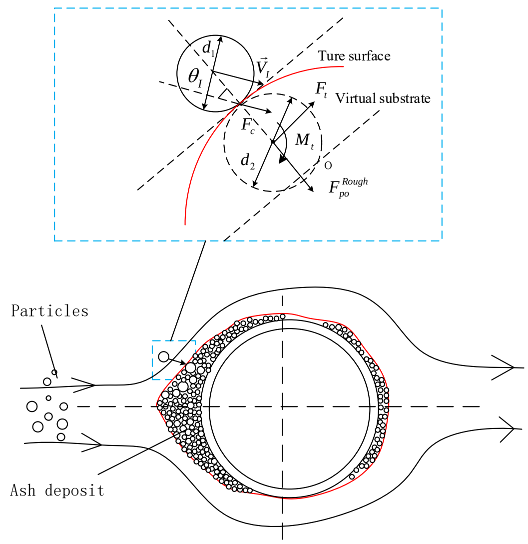

Fig. 4 Formation of ash deposit coupling processes of ash deposition and removal

which an incident particle collides with. A virtual substrate is also assumed to exist and support the adhered particle. The analysis of the forces and moment is done, similar to that in Fig. 3. With respect to the point O, a new criterion of rolling particle detachment is given as:

$$M_t + F_t(\frac{d_2}{2} - a_0) + F_l\alpha_{Rough} + F_c[\sin\theta_I(d_2 - a_0) - \cos\theta_I\alpha_{Rough}] \geq F_{po}^{Rough}\alpha_{Rough} \quad (14)$$

Accordingly, a new criterion of sliding particle detachment is given as:

$$F_t + F_c\sin\theta_I \geq (F_{po}^{Rough} - F_l + F_c\cos\theta_I) f_s \quad (15)$$

3. CASE STUDY

3.1 Mesh and boundaries

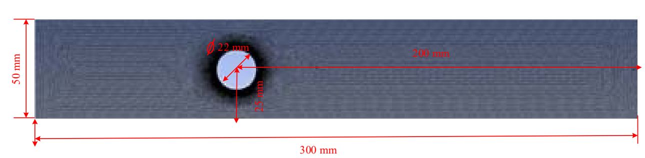

Fig. 5 The geometry and grid of the computational domain

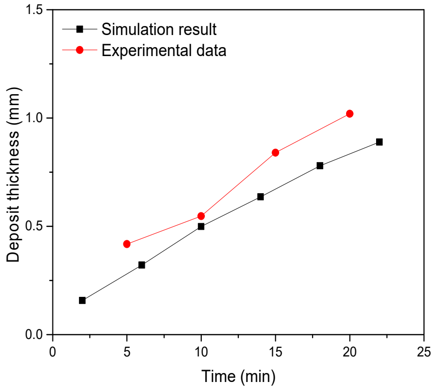

Fig. 7 Comparisons of the deposit thicknesses over time between the simulation result and experimental data

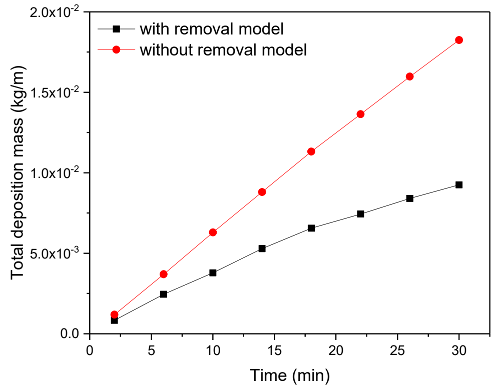

Fig. 8 Ash deposition mass over time with and without removal model for the case with the inlet velocity of 1.93 m/s

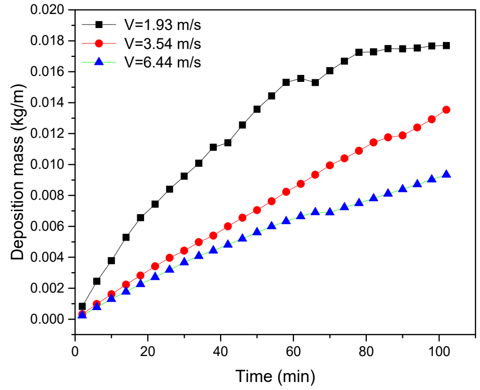

Fig. 9 The effects of flue gas velocity on ash deposition mass

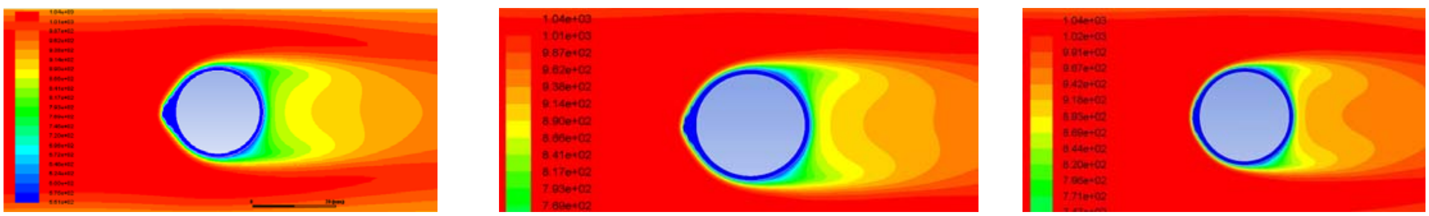

V=1.93 m/s V=3.54 m/s V=6.44 m/s

Fig. 6 The final morphologies of the fouling probe for three cases

The geometry and grid of the computational zone are shown in Fig. 5 The triangular grids were adopted in the computational zone to apply the dynamic mesh model. A fully fine grids approaching the deposition probe is required to accurately resolve the flow field within the boundary layer of this deposition surface, according to the suggestion of Weber et al. [15]. A fixed-type size function in Gambit was thereby applied to smoothly control the growth in mesh size and growth rate over the surface of the probe. The left boundary of the domain is set as the velocity inlet in the horizontal direction. The right boundary of the domain is set as the pressure outlet. The upper and lower boundaries of the as well as the deposition probe are wall boundaries. No slip condition is applied to them.

3.2 Simulation parameters

The important parameters used in this simulation are listed in Table 1.

4. RESULT AND DISCUSSION

4.1 Experimental validation

The deposition thicknesses as a function of time were compared between the simulation result and experimental data, as shown in Fig. 7. The result shows that the changing trends of the deposition mass for the simulation result and experimental data are consistent, but the discrepancy between them seems to be gradually increasing with time. One possible reason for this discrepancy is that Young's module of particles is taken as a constant in the simulation, but actually it depends on particle size, temperature, and chemical composition of particles. Unfortunately, presently there is no accurate data for this parameter for biomass ash.

4.2 Effect of removal model

The effect of ash deposition removal model was investigated by comparing the cases with and without the removal model, as shown in Fig. 8. The results show that the deposition mass increases linearly with time for the case without the removal model, but it presents an asymptotic trend for the case with the removal model. Furthermore, it is found that there is a significant difference between the cases with and without the removal model, and the difference are increasing with time. It means that it is necessary to consider the removal model when simulating the growth of ash deposit, even under the cases that the flue gas velocity is so low.

4.3 Effect of flue gas velocity

The flue gas velocity is an important factor affecting ash deposition. Therefore, the effect of the flue gas velocity on ash deposition was investigated, as shown in Fig. 9. The results show that the deposition mass decreases significantly with increase of the flue gas velocity. On the one hand, the increase of the flue gas velocity leads to the rebounces of more particles. On the other hand, the removal rate also increases with the increase of the flue gas velocity. The final morphologies of the fouling probe for three cases are shown in Fig. 6.

Table 1 Parameters for this simulation

Parameters	Values
Particle density	3100 kg/m^3
Young's module of particles	5.0E^6 Pa
Young's module of the stainless steel	2.0E^{11} Pa
Poisson's ratio of particles	0.3
Yield stress of particles	4.1E^8 Pa
Adhesion work of particles	0.3 J/m^2
Friction coefficient	0.7
Inlet temperature of particles	762 ℃
Velocities of particles	1.93, 3.54 and 6m/s
Particle concentration	0.006 kg/m3
Inlet temperature of flue gas	762 ℃
Velocities of flue gas	1.93, 3.54 and 6m/s
Max particle diameter	447 µm
Min particle diameter	2 µm
Avarage particle diameter	65 µm
Diffusion factor	1.04 µm

5. CONCLUSIONS

A mechanistic fouling model considering the build-up and removal mechanism was developed. Coupled with ANSYS FLUNET software by user defined codes, the fouling model was used to predict ash deposition behavior of woodchip ash. The results show reasonable agreement between experimental data and modeling results. It provides a predictive tool to model ash deposition behavior in low-temperature conditions for the woodchip fired boiler. The results show the removal mechanism plays an important role in ash deposition, even at the low flue gas velocity, it is necessary to consider the removal mechanism. The flue gas velocity is a key factor affecting ash deposition. The deposition mass decreases with the increase of flue gas velocity. The impact mass flux and deposition flux are decreasing as the deposit grows, which was caused by the change of deposit shape. Young's module of ash particles significantly affects ash deposition. It is important to obtain the temperature-dependent properties of Young's module of ash particles to improve the simulation accuracy.

ACKNOWLEDGEMENT

The research is supported by the National Research Foundation Singapore, Sembcorp Industries Ltd and National University of Singapore under the Sembcorp-NUS Corporate Laboratory.

REFERENCE

[1] Walsh PM, Sayre AN, Loehden DO, Monroe LS, Beér JM, Sarofim AF. Deposition of bituminous coal ash on an isolated heat exchanger tube: Effects of coal properties on deposit growth. Progress in Energy and Combustion Science. 1990;16:327-45.
[2] Brink A, Lindberg D, Hupa M, de Tejada ME, Paneru M, Maier J, et al. A temperature-history based model for the sticking probability of impacting pulverized coal ash particles. Fuel Processing Technology. 2016;141:210-5.
[3] García Pérez M. Modeling the effects of unsteady flow patterns on the fireside ash fouling in tube arrays of kraft and coal-fired boilers. Acta Universitatis Lappeenrantaensis. 2016.
[4] Zbogar A, Frandsen F, Jensen PA, Glarborg P. Shedding of ash deposits. Progress in Energy and Combustion Science. 2009;35:31-56.
[5] Zhimin Z, Hui W, Yongtie C, Xing W, Shaohua W. A novel method used to study growth of ash deposition and in situ measurement of effective thermal conductivity of ash deposit. Heat Transfer—Asian Research. 2018;47:271-85.
[6] Zheng Z, Wang H, Guo S, Luo Y, Du Q, Wu S. Fly Ash Deposition during Oxy-fuel Combustion in a Bench-Scale Fluidized-Bed Combustor. Energy & Fuels. 2013;27:4609-16.
[7] Zheng Z, Yang W, Cai Y, Xu M, Boon SK, Subbaiah P. Numerical investigation on ash deposition on the surface of tube bundle. Energy Procedia. 2017;143:336-41.
[8] Tong Z-X, Li M-J, He Y-L, Tan H-Z. Simulation of real time particle deposition and removal processes on tubes by coupled numerical method. Applied Energy. 2017;185:2181-93.
[9] van Beek MC. Gas-side fouling in heat-recovery boilers: Technische Universiteit Eindhoven; 2001.
[10] Konstandopoulos AG. Particle sticking/rebound criteria at oblique impact. Journal of Aerosol Science. 2006;37:292-305.
[11] Sommerfeld M, Huber N. Experimental analysis and modelling of particle-wall collisions. International journal of multiphase flow. 1999;25:1457-89.
[12] Heinl E, Bohnet M. Calculation of particle–wall adhesion in horizontal gas–solids flow using CFD. Powder Technology. 2005;159:95-104.
[13] Toscano C, Ahmadi G. Particle removal mechanisms in cryogenic surface cleaning. The Journal of Adhesion. 2003;79:175-201.